


Exploring beamline momentum acceptance for tracking respiratory variability in lung cancer proton therapy: a simulation study

Journal Article

Author(s):

Giovanelli, Anna Chiara; Köthe, Andreas; Safai, Sairos; Meer, David; Zhang, Ye; Weber, Damien Charles; Lomax, Antony John; [Fattori, Giovanni](#) 

Publication date:

2023-10-07

Permanent link:

<https://doi.org/10.3929/ethz-b-000634314>

Rights / license:

[Creative Commons Attribution 4.0 International](#)

Originally published in:

Physics in Medicine and Biology 68(19), <https://doi.org/10.1088/1361-6560/acf5c4>



PAPER

Exploring beamline momentum acceptance for tracking respiratory variability in lung cancer proton therapy: a simulation study

OPEN ACCESS

RECEIVED

14 January 2023

REVISED

7 August 2023

ACCEPTED FOR PUBLICATION

31 August 2023

PUBLISHED

22 September 2023

Original content from this work may be used under the terms of the [Creative Commons Attribution 4.0 licence](#).

Any further distribution of this work must maintain attribution to the author(s) and the title of the work, journal citation and DOI.



Anna Chiara Giovannelli^{1,2,*}, Andreas Köthe^{1,2}, Sairos Safai¹, David Meer¹, Ye Zhang¹ , Damien Charles Weber^{1,3,4}, Antony John Lomax^{1,2} and Giovanni Fattori¹

¹ Center for Proton Therapy, Paul Scherrer Institute, 5232 Villigen, Switzerland

² Department of Physics, ETH Zürich, 8092 Zürich, Switzerland

³ Department of Radiation Oncology, University Hospital of Zürich, 8091 Zürich, Switzerland

⁴ Department of Radiation Oncology, Inselspital, Bern University Hospital, University of Bern, Switzerland

* Author to whom any correspondence should be addressed.

E-mail: anna-chiara.giovannelli@psi.ch

Keywords: proton therapy, tumour tracking, organ motion, momentum acceptance, 4D imaging, lung cancer, rescanning

Supplementary material for this article is available [online](#)

Abstract

Objective. Investigating the aspects of proton beam delivery to track organ motion with pencil beam scanning therapy. Considering current systems as a reference, specify requirements for next-generation units aiming at real-time image-guided treatments. **Approach.** Proton treatments for six non-small cell lung cancer (NSCLC) patients were simulated using repeated 4DCTs to model respiratory motion variability. Energy corrections required for this treatment site were evaluated for different approaches to tumour tracking, focusing on the potential for energy adjustment within beamline momentum acceptance (dp/p). A respiration-synchronised tracking, taking into account realistic machine delivery limits, was compared to ideal tracking scenarios, in which unconstrained energy corrections are possible. Rescanning and the use of multiple fields to mitigate residual interplay effects and dose degradation have also been investigated. **Main results.** Energy correction requirements increased with motion amplitudes, for all patients and tracking scenarios. Higher dose degradation was found for larger motion amplitudes, rescanning has beneficial effects and helped to improve dosimetry metrics for the investigated limited dp/p of 1.2% (realistic) and 2.4%. The median differences between ideal and respiratory-synchronised tracking show minimal discrepancies, 1% and 5% respectively for dose coverage (CTV V95) and homogeneity (D5-D95). Multiple-field planning improves D5-D95 up to 50% in the most extreme cases while it does not show a significant effect on V95. **Significance.** This work shows the potential of implementing tumour tracking in current proton therapy units and outlines design requirements for future developments. Energy regulation within momentum acceptance was investigated to tracking tumour motion with respiratory-synchronisation, achieving results in line with the performance of ideal tracking scenarios. $\pm 5\% \Delta p/p$ would allow to compensate for all range offsets in our NSCLC patient cohort, including breathing variability. However, the realistic momentum of 1.2% dp/p representative of existing medical units limitations, has been shown to preserve plan quality.

1. Introduction

Radiation therapy is a major player in the therapeutic armamentarium for the treatment of lung cancer (Liao and Simone 2018). Hence the importance of refining the treatment technique for this type of cancer which, due to its location in a region prone to organ motion, is challenging to treat. Moreover, sensitive organs at risk (OAR) must be taken into account when treating this area, such as healthy lung tissue, oesophagus, heart, spinal cord and bone marrow. In this regards, pencil beam scanning (PBS) proton therapy is a potentially prime option to

minimise off-target radiation delivery and thus reduce the risk of induced toxicities and ultimately improve clinical outcome of lung cancer patients. The most intuitive way to reduce dose to healthy tissues is to track the tumour position in real time with the treatment field, an approach that however brings additional challenges related to image guidance and online dose delivery control. Indeed tumour tracking is only available on a few advanced photon therapy units (Hoogeman *et al* 2009, J-Y *et al* 2008, Depuydt *et al* 2014). In a moving anatomy, controlling the range of protons and the interplay between the scanning beam and the target (i.e. interplay effect) are two key issues that have in fact held back the clinical translation of tumour tracking with protons, and charged particles therapy in general (Fattori *et al* 2017). In these modalities, a thin pencil beam is scanned across the target volume to deliver dose as a sequence of individual spots, organised in layers at different depths. While the lateral position of dose spots can be adjusted quickly by the scanning magnets, their position in depth is a function of the beam energy. The energy modulation process, most often including the insertion of degrading material in the beam, has generally latencies not compatible with on-line adaptation in clinical units, ranging from hundreds of milliseconds up to a few seconds (Giovannelli *et al* 2022). Although having a fast downstream energy degrader (Weber *et al* 2000) has been investigated in the context of tumour tracking (Bert and Durante 2011), such bulky equipment has never made the translation into clinical units. Our aim is therefore to explore an alternative option, one that does not require the installation of dedicated hardware and that is potentially far-reaching for clinical departments.

The limit to fast energy modulation is typically the tuning of the last bending dipole magnets for gantry based systems (Fattori *et al* 2020). This limitation can however be overcome for small changes of energy: in an achromatic beamline, particles with non-nominal momentum can be transported without chromatic dispersion within a determined range of acceptance (Fattori *et al* 2020, Giovannelli *et al* 2022). This momentum acceptance (dp/p) is specific to each treatment unit, but generally is of the order of 1%–2% dp/p (Yap *et al* 2021). In fact, ultra-fast energy regulation within 1.2% dp/p has been experimentally investigated by Giovannelli *et al* in a medical beamline and pencil beam properties confirmed to meet clinical standards (Giovannelli *et al* 2022). In our study we leverage such beamline momentum acceptance for tracking of non-small cell lung cancer tumours. Due to this finite acceptance, a number of simplifications are proposed to the conventional concept of tumour tracking, including the pre-optimisation of beam offsets to be delivered in synchrony with the patient breathing. The realism of our simulations is however ensured by the use of realistic breathing patterns, including respiratory variations from repeated 4DCT imaging of a number of cancer patients.

2. Methods

2.1. Modelling of respiratory variability

In this study, we considered six stage IIA–IIIA–IIIB non-small cell lung cancer (NSCLC) patients with tumours located in different lobes and all with repeated 4D imaging (Hugo *et al* 2017). From these, so-called ‘multi-breath 4DCT images’ (m4DCT) have been generated, which include a wide range of tumour motion amplitudes and volume deformations (Giovannelli *et al*). m4DCT data is generated by transferring the motion description derived from repeated 4DCT images onto the planning CT in a process summarised in figure 1. For this work, five breathing cycles from five 4DCTs were combined for each patient to model respiratory variability during treatments. For each patient, the mid-position (MP) image (Wolthaus *et al* 2008) is computed (Velocity version 4.1, Varian Medical Systems, Palo Alto, CA, USA) for the planning 4DCT (p4DCT) and for the repeated 4DCTs (r4DCTs), acquired for the same patient on different days. Such MPs are then used to establish the relation between the p4DCT and the r4DCTs. The breathing motion of each r4DCT is modelled by means of deformable image registration between the r4DCT-MP and its breathing phases (r4DCT-BP). Once deformable image registration between (i) p4DCT-MP and r4DCT-MP, and (ii) r4DCT-MP and r4DCT-BP are computed, the resulting vectors field from (i) are used to warp (ii) onto the p4DCT-MP, thus transferring the motion from r4DCTs onto the planning CT image to generate the breathing phases of the m4DCT. Note, this transfer of motions from each repeat CT to the planning CT is performed to mitigate the effect of anatomical changes that may have occurred between the time of the planning and repeat 4DCT’s. More information on this process can be found in the supplementary material.

2.2. Patient dataset

Clinical details and motion information for all patients are summarised in table 1. For each patient and all respiratory cycles, the deformable image registration statistics have been used to assess tumour motion and tumour volume deformation by analysing the GTV center-of-mass position and the vector field’s Jacobian determinant maps (Fiorino *et al* 2011).

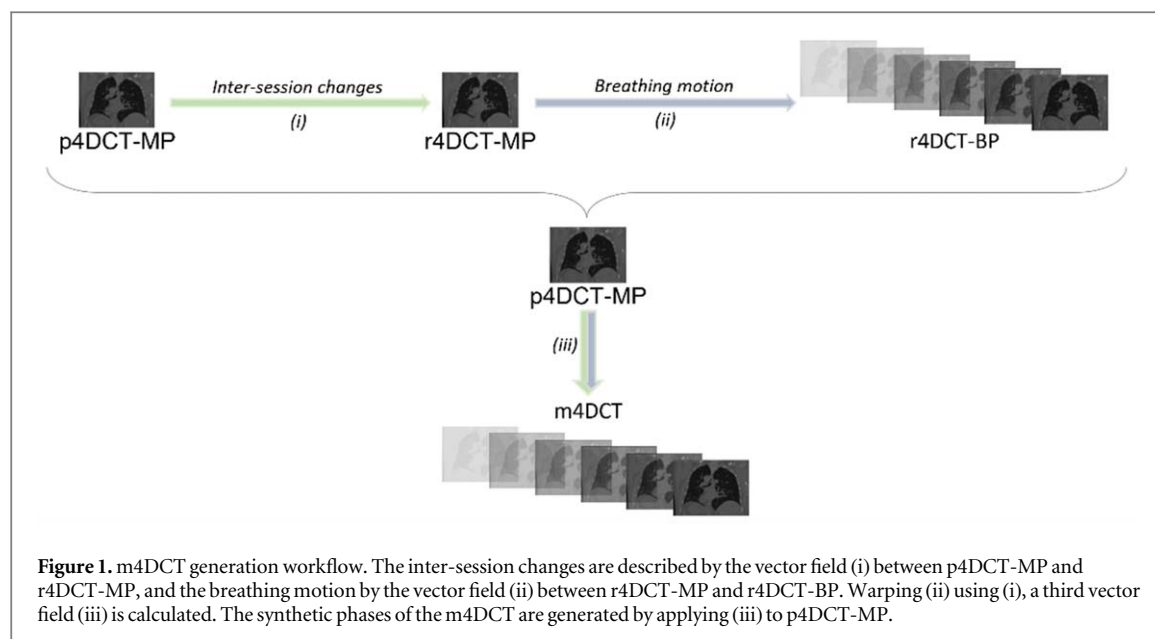


Table 1. Clinical and tumour motion characteristics of the NSCLC patients included in this study. The gross target volume (GTV) maximum variation is evaluated as the ratio between the volume of the tumour undergoing expansion or shrinkage respectively for inhale or exhale phases. The maximum value between the two variations has been reported. The median value of motion amplitude in the superior-inferior direction together with its maximum variation, as the delta between the maximum and the minimum amplitude with respect to the median.

Patient #	UICC stage	Location	GTV [mm ³] size (max variation)	Amplitude sup-inf [mm] median (max variation)
1	III A	left-upper	18 (91%)	2.4 (54%)
2	III A	right-upper	31 (67%)	0.4 (150%)
3	II A	left-lower	78 (74%)	7 (21%)
4	III A	right lower	179 (57%)	11.1 (78%)
5	III B	right-upper	7 (98%)	2.9 (41%)
6	III A	right-upper	10 (74%)	8.4 (74%)

2.3. Tumour tracking simulations

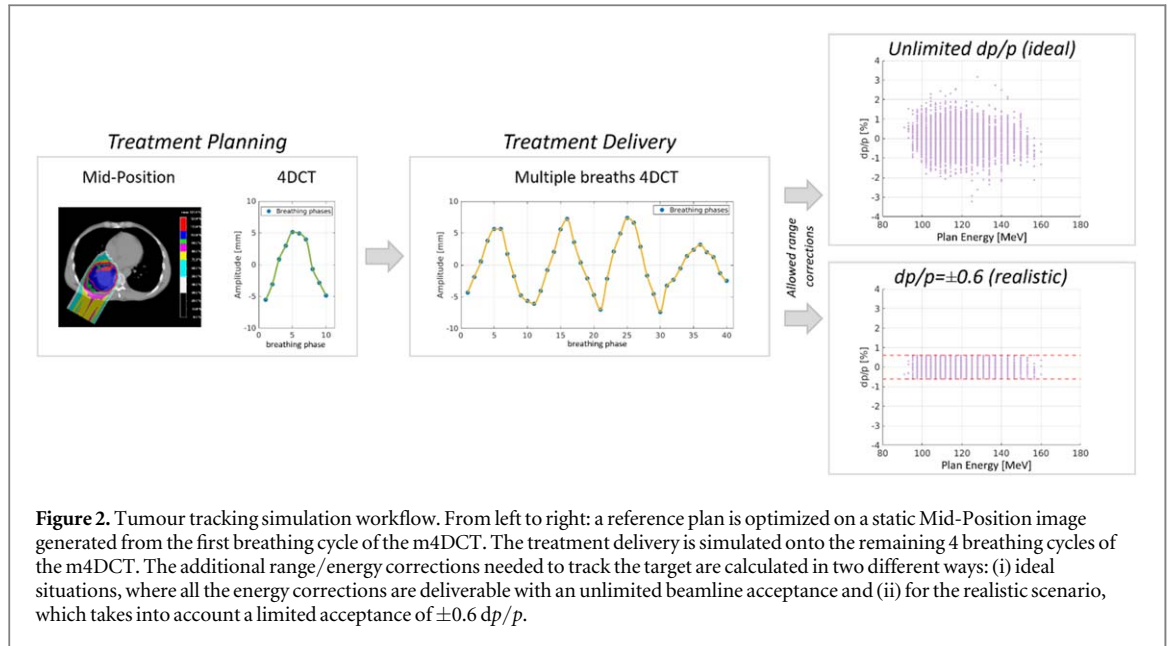
Reference plans were optimised for each patient on the mid-position image computed from the first breathing cycle of the m4DCTs (Wolthaus *et al* 2008, Bellec *et al* 2020) to deliver 1.8 GyRBE_{1.1} fraction dose. The gross tumour volume (GTV), delineated by an experienced radiation oncologist (Hugo *et al* 2017), was first isotropically expanded by 5 mm to the clinical volume (CTV) and subsequently grown to obtain the planning target volume (PTV) as follows (Roelofs *et al* 2012):

$$\text{Margins}_{\text{CTV to PTV}} = 2.5 \Sigma + 0.7 \sigma \sim 7 \text{ mm}$$

Σ and σ represent systematic and random components that model patient positioning errors and range uncertainties. We considered Σ and σ to be 2 and 3 mm respectively (Köthe *et al* 2022).

The remaining four breathing cycles of each m4DCT dataset have been used to simulate the delivery under realistic clinical conditions of variable respiratory motion. We will refer to this dataset as *delivery-m4DCT*. The workflow is summarised in figure 2.

In this study we have compared two approaches to tumour tracking, in the following referred to as (i) *ideal tracking* and (ii) *respiratory-synchronised tracking*, assuming either unlimited or (currently) realistic beam acceptances. 4D dose calculations were performed (Boye *et al* 2013) considering a fixed breathing period between phases (500 ms), and with beam model and delivery parameters from our facility records (Pedroni *et al* 2004, Giovannelli *et al* 2022) featuring 1.2% dp/p acceptance. Lateral corrections have been assumed to be instantaneous, due to the high speed of the lateral scanning magnets (1 cm ms⁻¹) (Klimpki *et al* 2018), and the energy switching time considered to be 27 ms when modulated within acceptance (Giovannelli *et al* 2022), and 100 ms when modulated otherwise (Pedroni *et al* 2004). The possibility to include rescanning in the simulations has also been investigated, as an option to attenuate sensitivity and the uncertainties of pure tumour tracking (Van De Water *et al* 2009, Knopf *et al* 2011, Zhang *et al* 2014, Fattori *et al* 2020).



2.3.1. Ideal tracking

In the ideal tracking scenario, unconstrained energy corrections are allowed and can be applied in any direction, increasing or reducing the beam energy as needed. Such an ideal situation, disregarding beamline ramping and magnet hysteresis, somewhat replicates a setup with an arbitrarily fast downstream energy degrader, and the energy switching time was assumed to always be as fast as 27 ms. On-the-fly corrections are calculated from the reference plan for each pencil beam to track the deforming anatomy modelled in the delivery-m4DCT images.

2.3.2. Respiratory-synchronised tracking

In respiratory-synchronised tracking, a pre-optimisation based on the planning 4DCT is required. Following the method of (Fattori *et al* 2020), the scan path does not follow the conventional sequence of iso-energy layers, but the spot list is altered to make use of the beamline acceptance and to achieve fast energy modulation. From 230 MeV down to 70 MeV, 54 energy bands of width equal to the acceptance (1.2% dp/p) are defined, within which range corrections as fast as 27 ms can be set without changes in the beamline energy tune, otherwise considered to be 100 ms. In this work the standard high-to-low ramping scheme has been used, guiding the selection of the starting breathing phase to be the one with the highest beam energy. Starting from this first spot, the algorithm progressively builds the scan path. Spots are re-sorted to maintain a continuous progression of energies (descending or ascending order) including the tracking offsets required to synchronise the delivery with the sequence of breathing phases. Starting from a reference plan, each spot is defined by XY lateral coordinates and an energy E , which can be converted into water equivalent range (WER) coordinate, Z_{WER} :

$$X [\text{cm}], Y [\text{cm}], E[\text{MeV}] \xrightarrow{\text{from energy to WER}} X [\text{cm}], Y [\text{cm}], Z_{\text{WER}} [\text{cm}]$$

The water equivalent range Z_{WER} needs to be converted into the actual spot position Z_{CT} in the CT image. Once all the coordinates are defined as such in the reference plan, the spot position can be warped by deformable image registration (DIR) to define the position $X'Y'Z'_{\text{CT}}$ in the 4D breathing phase:

$$Z_{\text{WER}} [\text{cm}] \xrightarrow{\text{from WER to CT coordinates}} Z_{\text{CT}} [\text{cm}]$$

$$X [\text{cm}], Y [\text{cm}], Z_{\text{CT}} [\text{cm}] \xrightarrow{\text{DIR}} X' [\text{cm}], Y' [\text{cm}], Z'_{\text{CT}} [\text{cm}]$$

The deformed spot range position Z'_{CT} is converted back into WER Z'_{WER} , and subsequently into energy E' . Once the energy in the 4D phase is defined, the spot can be resorted and placed within the correct energy band:

$$Z'_{\text{CT}} [\text{cm}] \xrightarrow{\text{from WER to CT coordinates}} Z'_{\text{WER}} [\text{cm}] \xrightarrow{\text{from WER to energy}} E' [\text{MeV}] \xrightarrow{\text{resorting}} E_{\text{band}}$$

On-the-fly lateral and energy corrections are then calculated by comparison between such an energy-resorted spot list and the further offsets necessary to track the delivery-m4DCT, thus adapting the plan to the actual patient breathing.

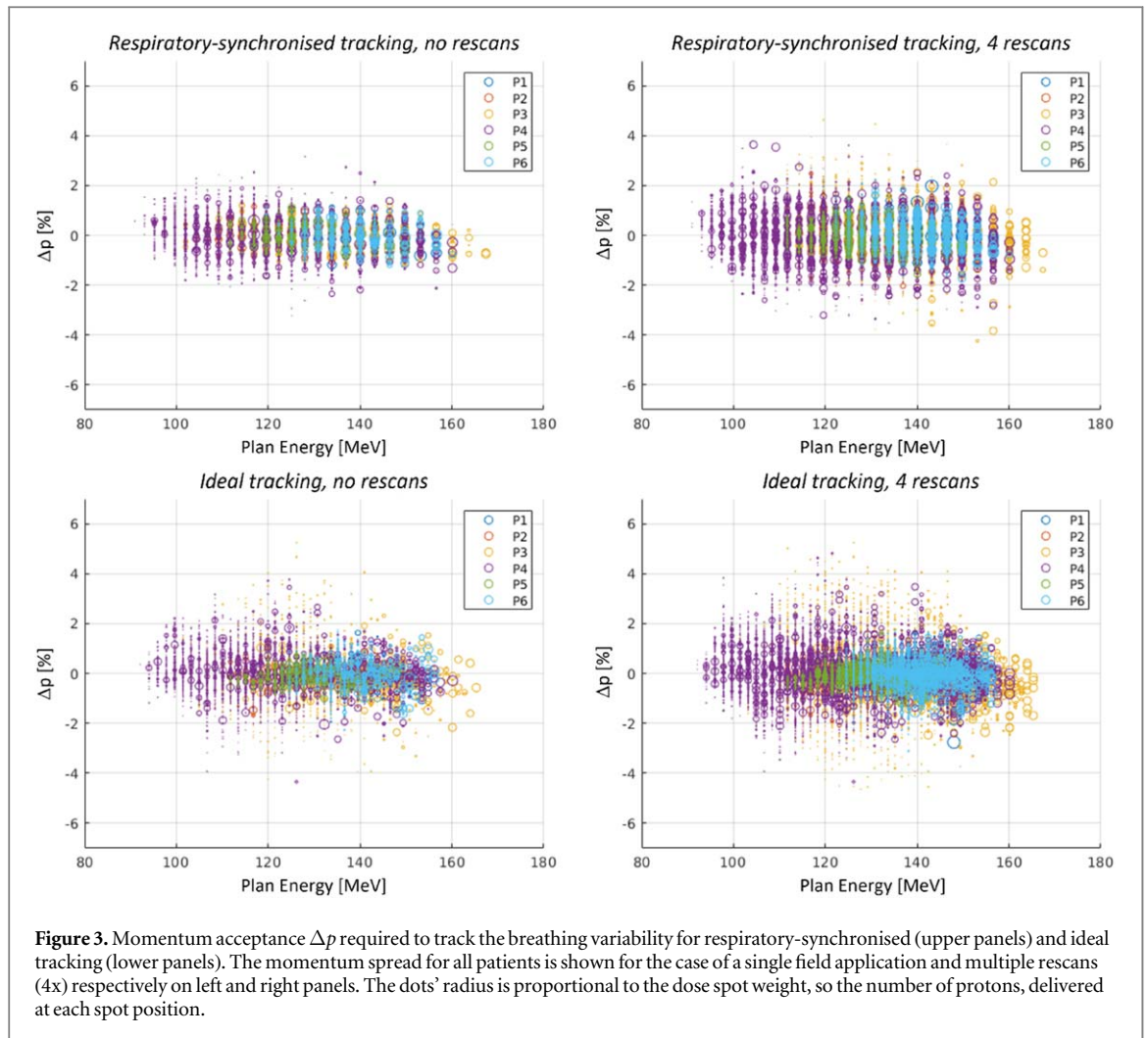


Figure 3. Momentum acceptance Δp required to track the breathing variability for respiratory-synchronised (upper panels) and ideal tracking (lower panels). The momentum spread for all patients is shown for the case of a single field application and multiple rescans (4x) respectively on left and right panels. The dots' radius is proportional to the dose spot weight, so the number of protons, delivered at each spot position.

2.3.5. Treatment plan evaluation

Ideal and respiration-synchronised tracking treatments have been simulated for all patients, using PBS and up to 4 volumetric rescans (RS), a value generally considered to be the limit for clinical therapy units when irradiation time and dose monitor performance are taken into account (Köthe *et al* 2022). Moreover, the alternative use of multiple uniform dose fields, as an alternative to rescanning (Knopf *et al* 2011) was investigated by considering up to three fields for the treatment of the two patients with the largest motion amplitudes (P4 and P6).

The corrections of dose spot positions to track the delivery-m4DCT can be converted to energy offsets, and thus to deltas of the momentum acceptance Δp required in the beamline. Δp has been calculated for all the patients and both tumour tracking strategies. To simulate a realistic scenario, a limit has been applied to the maximal energy correction allowed for respiratory-synchronised tracking at 1.2% ($\pm 0.6\%$) dp/p and at 2.4% ($\pm 1.2\%$) dp/p . However, and as shown in figure 2, we have also simulated what would be possible with an unconstrained acceptance. Motion-induced dose degradation was assessed from dose-volume-histograms (DVH) metrics (ICRU 2007), quantifying target dose coverage and homogeneity, respectively as CTV V95 and D5-D95 (Fattori *et al* 2019).

3. Results

For both ideal and respiratory-synchronised tracking, momentum requirements grow as a function of motion amplitude and its variability (figure 3). In our dataset, maximum/minimum (IQR) Δp ranged from 0.8%/−0.3% (0.26%) and 1.16%/−1.17% (0.58%) of P2 (smallest motion) to 3.77%/−4.34% (0.7%) and 3.15%/−3.2% (0.76%) for the largest motion (P4), for ideal and respiratory-synchronised tracking respectively. This spread increases when using rescanning for all patients and for both tracking scenarios (figure 2). In particular, with 4 times rescanning and respectively for ideal and respiratory-synchronised tracking, the Δp increases up to 1.37%/−2.08% (0.26%) and 2.48%/−2.64% (0.61%) for P2, and to 4.82%/−4.33% (0.71%) and 3.64%/−3.51% (0.78%) for P4.

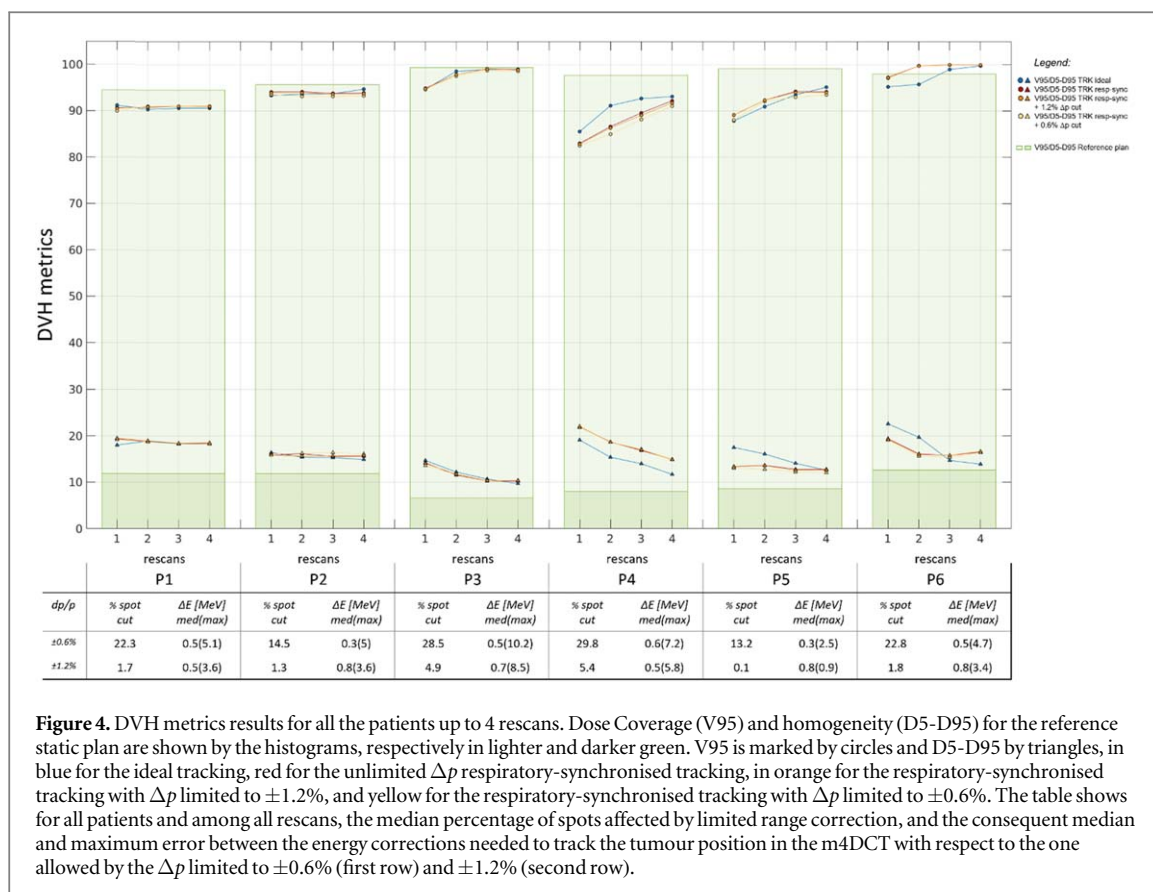


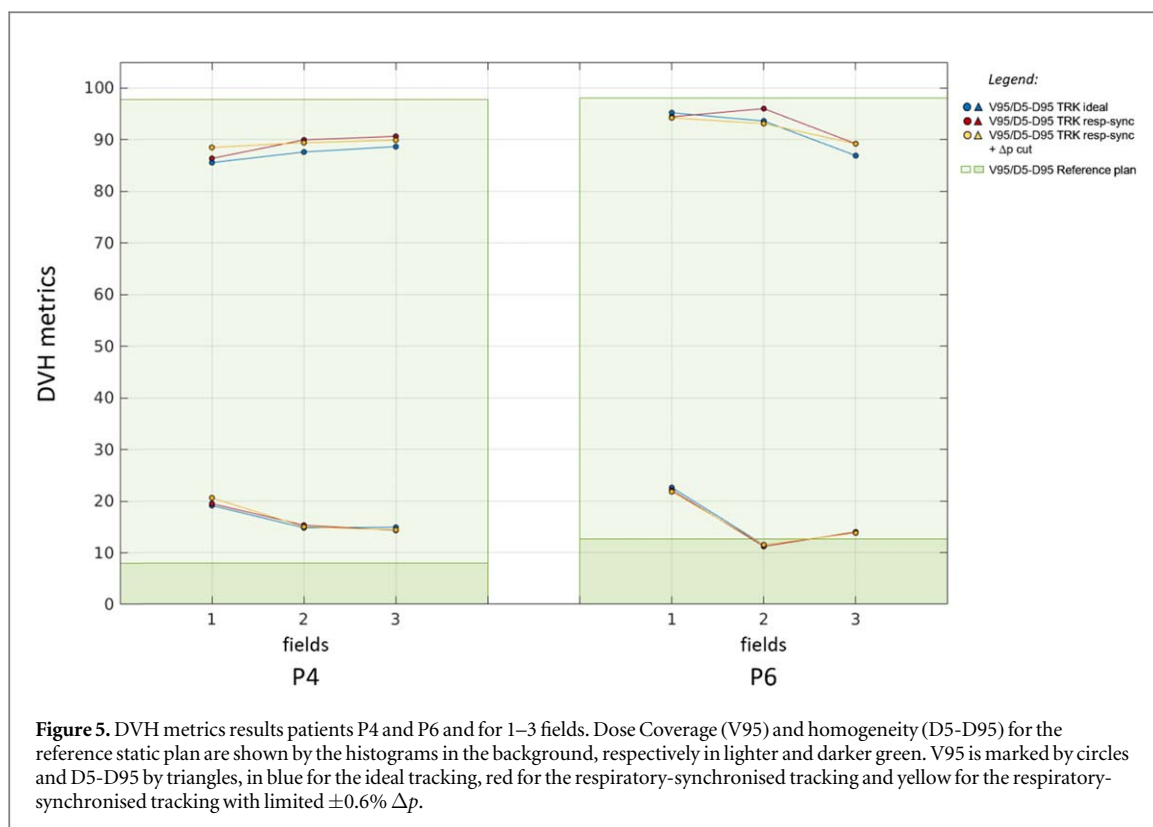
Figure 4. DVH metrics results for all the patients up to 4 rescans. Dose Coverage (V95) and homogeneity (D5-D95) for the reference static plan are shown by the histograms, respectively in lighter and darker green. V95 is marked by circles and D5-D95 by triangles, in blue for the ideal tracking, red for the unlimited Δp respiratory-synchronised tracking, in orange for the respiratory-synchronised tracking with Δp limited to $\pm 1.2\%$, and yellow for the respiratory-synchronised tracking with Δp limited to $\pm 0.6\%$. The table shows for all patients and among all rescans, the median percentage of spots affected by limited range correction, and the consequent median and maximum error between the energy corrections needed to track the tumour position in the m4DCT with respect to the one allowed by the Δp limited to $\pm 0.6\%$ (first row) and $\pm 1.2\%$ (second row).

Similarly, dose homogeneity and coverage worsen as a function of motion, with lower values for the patient with larger breathing amplitudes P4. Respiratory-synchronised and ideal tracking however follow a similar trend (figure 4), which proves rescanning to be beneficial.

Limiting the dp/p , and thus the energy correction that is achievable, results in a number of spots being delivered under suboptimal conditions. As shown in figure 4 for a dp/p of 1.2%, the correction of up to 30% of the plan spots is limited to the acceptance boundary for patients with larger breathing amplitudes (e.g. P4), a value that decreases to 13% for P2 with smaller breathing amplitudes. Allowing for 2.4% dp/p , more spots are correctly delivered to track the m4DCT, and these values consequently decrease down to 5% and 1.4%, for P4 and P2 respectively. With unlimited acceptance, target coverage and dose homogeneity for a single scan, with either ideal or respiratory-synchronised tracking were not statistically different at the 5% confidence level (Friedman p -value = 0.65 and p -value = 0.65) for V95 and D5-D95 respectively. No statistical significance was found between the dosimetry metrics under consideration when comparing synchronised deliveries including 1.2% and 2.4% dp/p (V95 p = 0.18, D5-D95 p = 0.37), and without or with an acceptance limit for synchronised deliveries (p = 0.18 and p = 0.82). Similarly, taking rescanning into account, no statistical differences were found between ideal and synchronised tracking (p = 0.6 and p = 0.89) or between synchronised tracking with or without a momentum limitation (p = 0.30 and p = 0.70). Once again, the two extreme cases in terms of motion amplitude (P2 and P4) nicely illustrate these trends. In absence of rescanning, we obtained V95/D5-D95 of 93.3%/16.4% (P2) and 85.6%/19.1% (P4) for ideal tracking, and 94.1%/15.9% (P2) and 83%/22% (P4) using breathing synchronization.

Rescanning (4x) brings dosimetry closer to those of stationary conditions (95.7%/11.9% and 97.7%/8%): 93.9%/15.6% and 92.2%/15% for the respiratory-synchronised tracking and 94.7%/14.9% and 93.1%/11.7% for ideal tracking. When limiting the acceptance, the same trend is followed, bringing dosimetry to 93.3%/16.2% (P2) and 91.0%/15% (P4), and 93.7%/15.8% (P2) and 91.7%/14.9% (P4) respectively for momentum acceptances limited to 1.2% and 2.4% dp/p .

Both patients with the largest motion amplitudes were finally replanned with multiple fields, without rescanning and using clinically available acceptances. Up to three fields have been used in the simulations of P4 and P6 treatments, and have been simulated using similar tumour tracking scenarios and with momentum acceptance limited to 1.2% dp/p (figure 5). Dose homogeneity improves when compared to the single field case, reducing for the respiratory-synchronised tracking with the limited acceptance from 20.6% and 21.8% to 14.4%



and 13.8% respectively for P4 and P6 when 3 fields are considered. V95 instead was not improved, going from 88.5% and 94.2% to 89.9% and 89.2% for one and three field plans respectively.

4. Discussion

In our analysis, by utilising the momentum acceptance of a clinical beam line, tumour tracking of lung tumours with protons has been simulated in combination with rescanning under realistic breathing scenarios and for different beamline capabilities. We used repeated time-resolved 4D imaging to model respiratory variability and thus assess the robustness of tumour tracking with respect to organ motion, an approach that goes beyond the clinical standard of a single planning 4DCT and the associated limitations for motion modelling. To our knowledge, the novel, patient specific m4DCT generation approach described in our study is one of its kind. Irregular breathing patterns, are most often reproduced by generating synthetic CT images that model the motion of healthy volunteers (Krieger *et al* 2020). Moreover, we observe an overestimation of motion respiratory amplitudes when comparing our study, completely relying on clinical images from lung cancer patients, to those with motion extracted from healthy volunteers. In addition, an ideal tracking approach simulating a next-generation beamline with unlimited acceptance, or a downstream degrader setup, has also been simulated, a scenario where arbitrary changes in beam energy are allowed.

In respiratory-synchronised tracking, spots are corrected on prior motion knowledge and sorted to comply with the conventional progression of beam energies while leveraging momentum acceptance for continuous regulation. To our knowledge, there are no publications investigating such use of momentum acceptance to perform fast energy modulation following irregular breathing, while also considering the performance of existing pencil-beam proton therapy facilities and defining requirements for future ones. In our approach, the spot delivery sequence is optimised to the breathing phases of the planning 4DCT to achieve the best tracking conditions in terms of energy corrections, while considering the interplay between respiratory motion and beam position. In this case, we have also investigated the impact of a realistic limitation in momentum acceptance when tracking motion with amplitude variability. The median differences between dose coverage and homogeneity for the two tracking strategies were 1% and 5% respectively, a minimal discrepancy that corroborates the clinical potential of respiratory synchronized tracking. In this work, a standard high-to-low energy progression has been studied. However, the possibility to re-start the delivery with a low-to-high energy sequence could be an interesting possibility to skip full magnet ramping between scans, thus shortening the delivery time and adding flexibility in the spot resorting optimisation (Actis *et al* 2018, Fattori *et al* 2020).

Organ motion has hereby been shown to amplify dose degradation, especially when the difference in motion between planning 4DCT and organ motion during delivery (delivery-m4DCT) leads to large range corrections. As shown in figure 2, patients with larger motion required up to $\pm 5\%$ Δp to fully cover the range of energy offsets required for tracking, a value that is beyond the specifications of existing facilities, but not far from what has been shown to be possible with super conducting magnets, where the momentum band can exceed $\pm 10\%$ dp/p (Nesteruk *et al* 2019, Yap *et al* 2021). By limiting the acceptance at 1.2% dp/p however, we have investigated what is achievable in most clinical facilities currently in operation, and by considering 2.4% dp/p we aimed to look into an intermediate situation, to question whether clinical level treatments could be achieved with momentum acceptance requirements in between those available in currently operating clinics and those under study for super conducting gantries. If on one hand, corrections are limited, energy modulation within acceptance would not require additional modifications of the beamline, while ensuring clinical level beam quality at isocenter (Giovannelli *et al* 2022). Moreover, within the momentum acceptance range, energy jumps are possible without re-tuning the magnets settings. The additional ability to deliver range corrections in both energy directions within acceptance would provide an extra degree of freedom which is particularly useful in the perspective of spot position adaptation in real time, and it would allow even a greater flexibility by the aforementioned large acceptance beamlines.

Tumour tracking is the most intuitive technique to mitigate organ motion, and it should in principle attenuate dose degradation due to the interplay with the scanned beam. However, it can suffer from the so-called inverse-interplay effect (Bert *et al* 2010, Zhang *et al* 2014) and, as shown by Bert and Rietzel (2007), there are many open challenges to be faced to fully recover target dose conformity and homogeneity in case of online adaptation. Different options have been explored to tackle these, like real-time dose compensation (Luchtenborg *et al* 2011) or 4D optimisation (Eley *et al* 2014). However, dose compensation is limited in presence of rotational/deformational motion, and 4D optimisation is time-consuming and challenging to be applied in real-time. Since no definitive answer exists to the aforementioned problems, and our focus is shifted towards the beam delivery aspects of tumour tracking, we investigated here the most simple approach of rescanning, as a way to mitigate dose degradations in the target and upstream tissues (Van De Water *et al* 2009, Fattori *et al* 2020, Krieger *et al* 2021) which has been demonstrated to reduce dose corruption and inhomogeneity, in particular in proximal tissue upstream of the target (Fattori *et al* 2020).

In agreement with the existing literature, dose coverage and homogeneity increase with the number of rescans for ideal and respiratory-synchronised tracking. The same conclusion holds true when beam acceptance limits the amount of energy modulation. In fact, even for a strict constrain of 1.2% dp/p , the number of spots delivered under suboptimal conditions is always below 30% of the total number of spots in the treatment plan, and for those, the median unapplied correction never exceeded 1 MeV. The maximum energy errors, shown in figure 4, significantly decrease for 2.4% dp/p , being up to 64% in the most extreme case (P5). However, the median errors do not show a substantial reduction. When assuming 1.2% dp/p , the energy errors are much greater in number and include many small corrections, leading to median energy corrections closer to the ones needed for 2.4% dp/p . Indeed, few spots are left outside the allowed energy corrections when 2.4% dp/p is considered, and in the most extreme case (P5) only one spot per rescan is delivered under suboptimal conditions. Multiple fields plans have also been investigated as an alternative to rescanning. Since the respiratory-synchronised delivery was able to recover the ideal tracking scenario with momentum restricted to 1.2% dp/p however, multiple field plan simulations have not been repeated for 2.4% dp/p . While the effect on dose coverage was not always beneficial, dose homogeneity always improved, reaching a gain close to 50% with respect to the single field plan in the most extreme cases.

Proton treatments of tumours affected by respiratory-induced organ motion are currently lacking a standard operation procedure, and being widely used in clinical practice, we decided to rely on the PTV concept and related margins in our plans' optimisation (Giaddui *et al* 2016). However, this practice has limitations, particularly when it comes to set-up and range uncertainties. Those are currently addressed by robust optimization techniques (Unkelbach *et al* 2018), and our study, which aims to be more a technical than a clinical study, can be viewed from a worst case scenario perspective in this context.

The accuracy of tumour tracking will also be dependent on the accuracy of motion estimations provided by on-line imaging. Proton radiography has been shown to provide a tool to model stopping power. However, even though a limited number of proton radiographies are shown to be able to sufficiently compensate for respiratory anatomical changes (Palaniappan *et al* 2021), the possibilities of applying the same approach to time resolved 4D images has not yet been demonstrated. It should be noted that, in our study, all tracking simulations have been performed assuming exact knowledge, in real time, of the actual patient deformation due to organ motion, and we therefore did not consider delay in the spots' delivery related to imaging and motion monitoring. However, to assess the position of the target, patient breathing needs to be monitored, processed and correlated to the actual target position and deformation, thus latencies have to be expected due to image processing

(Korreman 2015) and system readout (Fattori *et al* 2017). Even if these latencies can be as low as tens of milliseconds, they add to the uncertainty of tracking.

For imaging tumour motion, in room volumetric imaging technologies, such as 4D cone beam CT, magnetic resonance or optical systems, are relatively widespread, also in particle therapy, and could be important tools to create surrogate images to update patient anatomy information in synchrony with the treatment delivery (Zhang *et al* 2013, Landry and Hua 2018). However the translation of these techniques in particle therapy is still challenging: on board x-ray images and cone beam CTs expose the patient to additional ionising radiation dose (Korreman 2015) and respectively offer poor soft tissue contrast or are limited in 4D capabilities; magnetic resonance imaging does not add on dose, but needs complex magnet configurations and still requires conversion algorithm to obtain surrogate tissues' electron density information for beam adaptation (Pham *et al* 2022); and finally, optical tracking system are easy to integrate but require correlation models to estimate the internal target position from surface body motion (Pepin *et al* 2011). Garau *et al* proposed a novel ROI global motion model (Garau *et al* 2019) which, by coupling 4DCT and online MRI, aims to compensate for different anatomic-pathological structures while accounting for uneven respiratory motion. Even though these novel approaches are still far from a clinical translation and real-time performance, they are showing promising results for future applications.

5. Conclusions

The potential of using momentum acceptance for tumour tracking has been investigated taking into account the specifications of state-of-the-art proton therapy facilities. Clinical parameters have been evaluated considering a realistic model of the breathing variability and changes between planning and fraction days. Two different respiratory-synchronised tumour tracking strategies were compared to the ideal tracking scenario most commonly assumed in previous studies. Even considering currently realistic beamline the momentum acceptance (1.2% dp/p) as a limit in fast energy modulation, the clinical parameters for all techniques considered are comparable. Moreover, rescanning has been shown to improve the quality of respiratory-synchronised tracking, considering both constrained and unconstrained acceptance scenarios. The use of multiple fields, has been found also to help improve dose homogeneity.

In conclusion, based on our simulations, energy modulation within the momentum acceptance of a medical beamline is a promising method to bring tumour tracking particle therapy closer to clinical implementation. However, we acknowledge that its clinical realisation still requires reliable and accurate on-line and real-time imaging of anatomical changes.

Acknowledgments

This study was supported by the Swiss National Science Foundation with the Grant 185082 *New concept adaptive real time tumour tracking*, the Grant #2018-223 of the Strategic Focal Area *Personalized Health and Related Technologies (PHRT)* of the ETH Domain. We extend our gratitude to the anonymous reviewers, whose insightful feedback greatly enhanced the quality of our manuscript. Their rigorous analysis and constructive critiques have significantly improved this paper, making the peer review process an invaluable part of our work.

Data availability statement

The data cannot be made publicly available upon publication because the cost of preparing, depositing and hosting the data would be prohibitive within the terms of this research project. The data that support the findings of this study are available upon reasonable request from the authors.

ORCID iDs

Ye Zhang  <https://orcid.org/0000-0003-1608-4467>

References

- Actis O, Mayor A, Meer D and Weber D C 2018 Precise beam delivery for proton therapy with dynamic energy modulation *J. Phys. Conf. Ser.* **1067** 992002
- Bellec J, Arab-Ceschia F, Castelli J, Lafond C and Chajon E 2020 ITV versus mid-ventilation for treatment planning in lung SBRT: a comparison of target coverage and PTV adequacy by using in-treatment 4D cone beam CT *Radiat. Oncol.* **15** 54
- Bert C *et al* 2010 Dosimetric precision of an ion beam tracking system *Radiat. Oncol.* **5** 61

- Bert C and Durante M 2011 Motion in radiotherapy: Particle therapy *Phys. Med. Biol.* **56** 16
- Bert C and Rietzel E 2007 4D treatment planning for scanned ion beams *Radiat. Oncol.*
- Boye D, Lomax T and Knopf A 2013 Mapping motion from 4D-MRI to 3D-CT for use in 4D dose calculations: a technical feasibility study *Med. Phys.* **40** 61702
- Depuydt T et al 2014 Treating patients with real-time tumor tracking using the Vero gimbaled linac system: implementation and first review *Radiother. Oncol. J. Eur. Soc. Ther. Radiol. Oncol.* **112** 343–51
- Eley J G, Newhauser W D, Lichtenborg R, Graeff C and Bert C 2014 4D optimization of scanned ion beam tracking therapy for moving tumors *Phys. Med. Biol.* **59** 3431–52
- Fattori G et al 2017 Monitoring of breathing motion in image-guided PBS proton therapy: comparative analysis of optical and electromagnetic technologies *Radiat. Oncol.* **63** 12–63
- Fattori G et al 2019 The dependence of interplay effects on the field scan direction in PBS proton therapy *Phys. Med. Biol.* **64** 095005
- Fattori G, Zhang Y, Meer D, Weber D C, Lomax A J and Safai S 2020 The potential of Gantry beamline large momentum acceptance for real time tumour tracking in pencil beam scanning proton therapy *Sci Rep.* **10** 15325
- Fiorino C et al 2011 Introducing the Jacobian-volume-histogram of deforming organs: application to parotid shrinkage evaluation *Phys. Med. Biol.* **56** 3301–12
- Garau N et al 2019 A ROI-based global motion model established on 4DCT and 2D cine-MRI data for MRI-guidance in radiation therapy *Phys. Med. Biol.* **64** 45002
- Giaddui T et al 2016 Establishing the feasibility of the dosimetric compliance criteria of RTOG 1308: phase III randomized trial comparing overall survival after photon versus proton radiochemotherapy for inoperable stage II-IIIb NSCLC *Radiat. Oncol.* **11** 66
- Giovannelli A C et al 2021 Generation of synthetic multi-breaths 4DCT imaging to model irregular breathing
- Giovannelli A C et al 2022 Beam properties within the momentum acceptance of a clinical gantry beamline for proton therapy *Med. Phys.* **49** 1417–31
- Hoogeman M, Prévost J-B, Nuytens J, Pöll J, Levendag P and Heijmen B 2009 Clinical accuracy of the respiratory tumor tracking system of the cyberknife: assessment by analysis of log files *Int. J. Radiat. Oncol. Biol. Phys.* **74** 297–303
- Hugo G D et al 2017 A longitudinal four-dimensional computed tomography and cone beam computed tomography dataset for image-guided radiation therapy research in lung cancer *Med. Phys.* **44** 762–71
- ICRU 2007 Geometric terms and disem and dose-volume *J. ICRU* **7**(2) 83–94 International Commission of Radiation Units and Measurements
- Jin J-Y et al 2008 Use of the BrainLAB ExacTrac X-Ray 6D System in Image-Guided Radiotherapy *Med. Dos.* **33**
- Klimpki G et al 2018 The impact of pencil beam scanning techniques on the effectiveness and efficiency of rescanning moving targets *Phys. Med. Biol.* **63** 145006
- Knopf A C, Hong T S and Lomax A 2011 Scanned proton radiotherapy for mobile targets - The effectiveness of re-scanning in the context of different treatment planning approaches and for different motion characteristics *Phys. Med. Biol.* **56** 7257
- Korreman S S 2015 Image-guided radiotherapy and motion management in lung cancer *Br. J. Radiol.* **88** 20150100
- Köthe A et al 2022 The impact of organ motion and the appliance of mitigation strategies on the effectiveness of hypoxia-guided proton therapy for non-small cell lung cancer *Radiother. Oncol.* **176** 208–14
- Krieger M et al 2020 Impact of internal target volume definition for pencil beam scanned proton treatment planning in the presence of respiratory motion variability for lung cancer: a proof of concept *Radiother. Oncol. J. Eur. Soc. Ther. Radiol. Oncol.* **145** 154–61
- Krieger M et al 2021 Liver-ultrasound-guided lung tumour tracking for scanned proton therapy: a feasibility study *Phys. Med. Biol.* **66** 35011
- Landry G and Hua C 2018 Current state and future applications of radiological image guidance for particle therapy *Med. Phys.* **45** e1086–95
- Liao Z and Simone C B 2018 Particle therapy in non-small cell lung cancer *Transl. Lung Cancer Res.* **7** 141–52
- Lichtenborg R, Saito N, Durante M and Bert C 2011 Experimental verification of a real-time compensation functionality for dose changes due to target motion in scanned particle therapy *Med. Phys.* **38** 5448–58
- Nesteruk K P, Calzolaio C, Meer D, Rizzoglio V, Seidel M and Schippers J M 2019 Large energy acceptance gantry for proton therapy utilizing superconducting technology *Phys. Med. Biol.* (<https://doi.org/10.1088/1361-6560/ab2f5f>)
- Palaniappan P et al 2021 Deformable image registration of the treatment planning CT with proton radiographies in perspective of adaptive proton therapy *Phys. Med. Biol.* **66** 45008
- Pedroni E et al 2004 The PSI Gantry 2: a second generation proton scanning gantry *Z. Med. Phys.* **14** 25–34
- Pepin E W, Wu H, Zhang Y and Lord B 2011 Correlation and prediction uncertainties in the CyberKnife Synchrony respiratory tracking system *Med. Phys.* **38** 4036–44
- Pham T T et al 2022 Magnetic resonance imaging (MRI) guided proton therapy: a review of the clinical challenges, potential benefits and pathway to implementation *Radiother. Oncol.* **170** 37–47
- Roelofs E et al 2012 Results of a multicentric in silico clinical trial (ROCOCO): comparing radiotherapy with photons and protons for non-small cell lung cancer *J. Thorac. Oncol. Off. Publ. Int. Assoc. Study Lung Cancer* **7** 165–76
- Unkelbach J et al 2018 Robust radiotherapy planning *Phys. Med. Biol.* **63** 22TR02
- Van De Water S, Kreuger R, Zenklusen S, Hug E and Lomax A J 2009 Tumour tracking with scanned proton beams: assessing the accuracy and practicalities *Phys. Med. Biol.* **54** 21
- Weber U, Becher W and Kraft G 2000 Depth scanning for a conformal ion beam treatment of deep seated tumours *Phys. Med. Biol.* **45** 12
- Wolthaus J W H, Sonke J J, van Herk M and Damen E M F 2008 Reconstruction of a time-averaged midposition CT scan for radiotherapy planning of lung cancer patients using deformable registration *Med. Phys.* **35** 3998–4011
- Yap J et al 2021 Future developments in charged particle therapy: improving beam delivery for efficiency and efficacy *Front. Oncol.* **11** 2234–943X
- Zhang Y, Knopf A, Tanner C, Boye D and Lomax A J 2013 Deformable motion reconstruction for scanned proton beam therapy using on-line x-ray imaging *Phys. Med. Biol.* **58** 8621–45
- Zhang Y, Knopf A, Tanner C and Lomax A J 2014 Online image guided tumour tracking with scanned proton beams: a comprehensive simulation study *Phys. Med. Biol.* **59** 24